

CLIPSelf fine-tunes CLIP ViTs by maximizing the cosine similarities between the region representations pooled from the dense feature map and the image representations of the corresponding image crops. The regions in our method can be obtained by partitioning an image into a grid of  $m \times n$  patches. The unique design of CLIPSelf eliminates the need for a complex region-text matching process or the acquisition of additional labeled region-text pairs while effectively bridging the gap between dense and image representations of the CLIP ViTs for region recognition. Consequently, CLIPSelf significantly strengthens the vision-language alignment of the CLIP ViTs' dense features, benefiting their application to downstream open-vocabulary dense prediction tasks.

However, when transferring the vision-language alignment of CLIP from global image representation to local region representation for the open-vocabulary dense prediction tasks, CLIP ViTs suffer from the domain shift from full images to local image regions. CLIPSelf, which adapts the image-level recognition ability of CLIP ViT to local image regions without needing any region-text pairs. CLIPSelf empowers ViTs to distill itself by aligning a region representation extracted from its dense feature map with the image-level representation of the corresponding image crop.

# CLIPSELF: VISION TRANSFORMER DISTILLS ITSELF FOR OPEN-VOCABULARY DENSE PREDICTION

Size Wu<sup>1</sup> Wenwei Zhang<sup>1</sup> Lumin Xu<sup>2</sup> Sheng Jin<sup>3,4</sup>

Xiangtai Li<sup>1</sup> Wentao Liu<sup>3,5</sup> Chen Change Loy<sup>1</sup>

<sup>1</sup> S-Lab, Nanyang Technological University

<sup>2</sup> The Chinese University of Hong Kong <sup>3</sup> SenseTime Research

<sup>4</sup> The University of Hong Kong <sup>5</sup> Shanghai AI Laboratory

## ABSTRACT

Open-vocabulary dense prediction tasks including object detection and image segmentation have been advanced by the success of Contrastive Language-Image Pre-training (CLIP). CLIP models, particularly those incorporating vision transformers (ViTs), have exhibited remarkable generalization ability in zero-shot image classification. However, when transferring the vision-language alignment of CLIP from global image representation to local region representation for the open-vocabulary dense prediction tasks, CLIP ViTs suffer from the domain shift from full images to local image regions. In this paper, we embark on an in-depth analysis of the region-language alignment in CLIP models, which is essential for downstream open-vocabulary dense prediction tasks. Subsequently, we propose an approach named CLIPSelf, which adapts the image-level recognition ability of CLIP ViT to local image regions without needing any region-text pairs. CLIPSelf empowers ViTs to distill itself by aligning a region representation extracted from its dense feature map with the image-level representation of the corresponding image crop. With the enhanced CLIP ViTs, we achieve new state-of-the-art performance on open-vocabulary object detection, semantic segmentation, and panoptic segmentation across various benchmarks. Models and code will be available at <https://github.com/wusize/CLIPSelf>.

## 1 INTRODUCTION

Dense prediction tasks, including object detection (Girshick, 2015; Ren et al., 2015) and segmentation (Hariharan et al., 2014; Kirillov et al., 2019b), have been significantly advanced in the era of deep neural networks. However, traditional detection and segmentation models are trained to recognize only a fixed set of object categories. Such a design restricts the real-world applications of these models where infinite visual concepts exist. Therefore, open-vocabulary object detection (Zareian et al., 2021) and image segmentation (Ghiasi et al., 2021), which require the detection and segmentation models to recognize and localize visual concepts unseen in the training datasets, are gaining increasing attention from the community.

Recent open-vocabulary approaches (Gu et al., 2021; Xu et al., 2022; Kuo et al., 2023; Xu et al., 2023b) are typically inspired by the Contrastive Language-Image Pre-training (CLIP) (Radford et al., 2021). As depicted in Fig. 1(a), CLIP models, particularly the variants incorporating vision transformers (ViTs), have demonstrated impressive generalization capabilities in image classification tasks, achieving exceptional zero-shot performance. To enable open-vocabulary object detection and segmentation, it is crucial to transfer the vision-language alignment of CLIP models, especially the powerful ViT-based variants, from full images to local image regions.

In light of this, we conducted a preliminary experiment to evaluate the region-language alignment of CLIP's dense features and assess their competence in local object recognition. As shown in Fig. 1(b), two approaches were tested using the region boxes annotated in the COCO dataset (Lin et al., 2014). The first approach, referred to as 'Image Crop', directly inputs the image crops that enclose the regions into CLIP and utilizes the image-level features for classification. The second

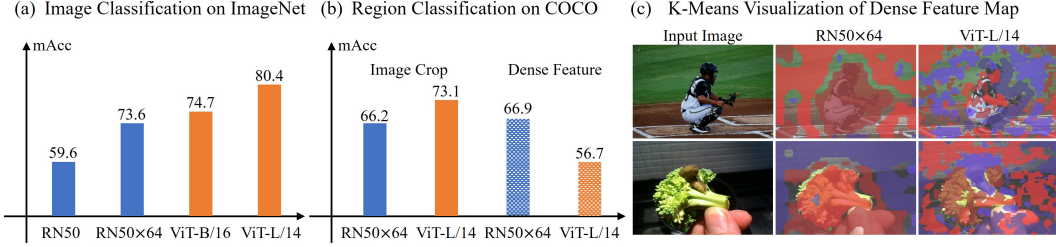


Figure 1: (a) CLIP ViTs exhibit excellent zero-shot ability on image classification compared with CLIP CNNs. (b) To classify regions, a CLIP ViT is as effective as a CLIP CNN by separately classifying the *image crop* of each region. However, it struggles when extracting region representation from the *dense feature* map for recognition. (c) The K-Means results of the CLIP ViT’s dense feature are much noisier, demonstrating the inferiority of CLIP ViT’s dense representation.

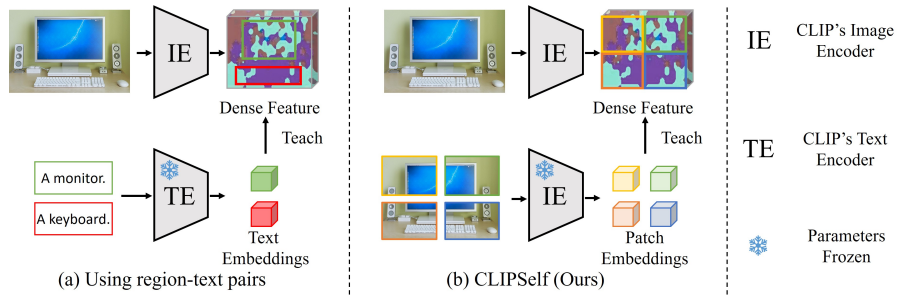


Figure 2: (a) Using region-text pairs to fine-tune CLIP for dense prediction tasks. These pairs are either manually annotated or generated via matching between region proposals and parsed image captions. (b) Our CLIPSelf does not rely on the association between text descriptions and regions, and only uses CLIP ViT’s representations of image patches to learn the dense features.

approach, referred to as ‘Dense Feature’, first obtains the dense feature map<sup>1</sup> of the input image and then extracts region representations from the feature map for recognition. Our findings reveal that the dense features of the Convolutional Neural Network (CNN) based model (RN50x64) exhibit high proficiency in region classification, surpassing the approach that uses image crops. This suggests the potential of directly applying CNN-based CLIP models to open-vocabulary dense prediction tasks. In contrast, the ViT-based model (ViT-L/14) struggles with region recognition when using its dense features, despite achieving satisfactory accuracy when utilizing image-level representations of the corresponding image crops. Furthermore, the K-Means visualization of the feature maps in Fig. 1(c) provides qualitative evidence of the inferior dense representation of ViT-based CLIP models. Compared to CNN models, CLIP ViT lacks local inductive bias, hindering the smooth transfer from representing pixels of a whole image to representing pixels of a local image region. More relevant analyses are provided in the appendix A.1. In recent years, notable progress has been made in building open-vocabulary object detectors based on frozen CLIP CNNs (Kuo et al., 2023; Wu et al., 2023c; Xu et al., 2023c), demonstrating competitive or state-of-the-art performance. However, applying CLIP ViTs to dense prediction tasks has proven challenging and less straightforward (Zhou et al., 2022a; Ding et al., 2023; Xu et al., 2023b). Therefore, we aim to develop an effective and general solution to address the limitations of CLIP ViTs’ dense representation.

One intuitive approach to enhance CLIP ViTs for dense prediction tasks involves fine-tuning CLIP using region-text pairs as illustrated in Fig. 2(a), which establishes a direct alignment between region and language representations. However, annotating sufficient region-text pairs for training a robust region representation is resource-intensive. To address this challenge, a recent work called Region-CLIP (Zhong et al., 2022) has explored the generation of pseudo labels by matching object nouns extracted from image captions with region proposals, thereby forming region-text pairs. While eliminating the need for exhaustive annotation, this approach suffers from the noisy matching between regions and object nouns. Compared with the probably imprecise text description (object noun) of a

<sup>1</sup>The dense feature map of a CLIP ViT is obtained following Zhou et al. (2022a), which modifies the output layer of ViT for better pixel-language alignment

region, the image-level representation of the image crop enclosing the region could serve as a more reliable teacher to guide the enhancement of the region representation in the context of CLIP ViTs as illustrated in Fig. 1.

In this paper, we present **CLIPSelf**, a self-distillation approach that obviates the necessity of paired data associating text descriptions with image regions. Fig. 2(b) provides an overview of how CLIP-Self derives a representation conducive to dense prediction through self-distillation. Specifically, CLIPSelf fine-tunes CLIP ViTs by maximizing the cosine similarities between the region representations pooled from the dense feature map and the image representations of the corresponding image crops. The regions in our method can be obtained by partitioning an image into a grid of  $m \times n$  patches. The unique design of CLIPSelf eliminates the need for a complex region-text matching process or the acquisition of additional labeled region-text pairs while effectively bridging the gap between dense and image representations of the CLIP ViTs for region recognition. Consequently, CLIPSelf significantly strengthens the vision-language alignment of the CLIP ViTs’ dense features, benefiting their application to downstream open-vocabulary dense prediction tasks.

The effectiveness of CLIPSelf is validated on open-vocabulary object detection and image segmentation benchmarks. For open-vocabulary object detection, we established a two-stage baseline based on frozen CLIP ViTs, and the fine-tuned models achieved state-of-the-art performance on OV-COCO and OV-LVIS benchmarks, as well as on the transfer detection benchmark. For open-vocabulary semantic and panoptic segmentation, CLIPSelf also yields non-trivial improvements to current state-of-the-art methods, such as Cat-Seg (Cho et al., 2023) and ODISE (Xu et al., 2023a).

## 2 RELATED WORK

**Open-Vocabulary Dense Prediction.** These directions primarily include object detection (Zareian et al., 2021; Gu et al., 2021; Kuo et al., 2023; Wu et al., 2023a), semantic segmentation (Xu et al., 2022; Ghiasi et al., 2021; Xu et al., 2023b), and panoptic segmentation (Xu et al., 2023a), aiming to recognize local visual concepts of arbitrary categories described by texts. This necessitates the alignment between region and text representations. The impressive vision-language alignment brought by Contrastive Image-Language Pre-training (CLIP) (Radford et al., 2021) has inspired numerous studies to explore the potential use of CLIP features for these tasks. For open-vocabulary detection, a series of works (Gu et al., 2021; Zang et al., 2022; Wu et al., 2023b) distill knowledge from the CLIP models to recognize novel objects. In contrast to distillation-based methods, F-VLM (Kuo et al., 2023) and CORA (Wu et al., 2023c) directly build object detectors upon frozen CLIP CNNs. For open-vocabulary segmentation, the typical two-stage approaches (Xu et al., 2022; Ding et al., 2022; Xu et al., 2023a) first generate class-agnostic mask proposals and then classify the proposals with CLIP. In particular, ODISE (Xu et al., 2023a) builds the mask generator upon frozen diffusion model (Rombach et al., 2022) and CLIP model. It fuses the CLIP score and the predicted score for classification in the inference stage. To validate the enhancement of CLIP ViTs’ dense representation by CLIPSelf, we build open-vocabulary object detectors upon frozen CLIP ViTs following F-VLM (Kuo et al., 2023). We also apply our refined models to open-vocabulary segmentation.

**Vision-Language Alignment for Images.** Vision-language pre-training has given rise to models with aligned image and text representations (Frome et al., 2013; Jayaraman & Grauman, 2014; Jia et al., 2021; Kim et al., 2021; Radford et al., 2021). Recent studies on contrastive vision-language pre-training (Jia et al., 2021; Radford et al., 2021; Zhai et al., 2022) have significantly improved the generalization ability of recognition models. In particular, CLIP models (Radford et al., 2021) that are pre-trained on billion-scale image-text pairs have exhibited impressive zero-shot classification performance on a wide range of datasets, among which the ViT-based variants are exceptionally powerful for image classification. However, alignment between visual content and language in CLIP’s ViT models is primarily constrained to the image level due to the lack of inductive bias by design and the absence of supervision on local image regions.

**Vision-Language Alignment for Regions.** Motivated by the success in aligning image and text representations, many studies (Zhong et al., 2022; Zhou et al., 2022a; Li et al., 2022a; Liu et al., 2023; Zhang et al., 2022; Mukhoti et al., 2023; Zou et al., 2023; Sun et al., 2023) have sought to achieve vision-language alignment at the local regions of images for dense prediction tasks. Some works (Zhong et al., 2022; Liu et al., 2023; Zhang et al., 2022) learn region-text alignment using annotations in visual grounding datasets (Krishna et al., 2017; Plummer et al., 2015) or generating

**pseudo-labeled region-text pairs.** And there are also weakly-supervised approaches (Gupta et al., 2020; Mukhoti et al., 2023) that indirectly align region and language representations using only image-text pairs. In addition to those relying on the paired data associating visual contents with text descriptions, **recent studies** (Zhou et al., 2022a; Ding et al., 2023) have attempted to preserve the CLIP ViTs’ vision-language alignment on the dense features by modifying the ViT’s output layer or employing masked attention. However, such attempts have yielded sub-optimal results due to the lack of inductive bias within CLIP ViTs and the absence of supervision on image regions. Different from these studies, our **CLIPSelf** facilitates the transfer of a CLIP ViT’s image-level vision-language alignment to local image regions by self-distillation, a process that circumvents associating regions with texts. Moreover, CLIPSelf is general and can be applied to open-vocabulary dense prediction tasks including object detection and image segmentation.

### 3 METHODOLOGY

We first introduce and analyze CLIP ViTs’ image and dense representations in Sec. 3.1. In Sec. 3.2, we introduce the proposed **CLIPSelf** that enhances CLIP ViTs’ dense representation without the need of region-text pairs. In Sec. 3.3, we introduce the applications of CLIPSelf to various open-vocabulary dense prediction tasks.

#### 3.1 IMAGE REPRESENTATION V.S. DENSE REPRESENTATION

A ViT-based CLIP model comprises a series of residual attention blocks. We briefly explain how the image and dense representations are obtained from the last residual attention block.

**CLIP’s Image Representation.** The input to the last residual attention block is  $\mathbf{x} = (x_0, x_1, \dots, x_{h \times w})^\top$  representing a class embedding  $x_0$  and  $h \times w$  image embeddings  $\{x_i | i \in \{1, 2, \dots, h \times w\}\}$ . A residual attention block  $\mathbf{z} = \text{ResAttn}(\mathbf{x})$  can be written as:

$$\begin{aligned} \mathbf{q} &= \text{Emb}_q(\mathbf{x}), \mathbf{k} = \text{Emb}_k(\mathbf{x}), \mathbf{v} = \text{Emb}_v(\mathbf{x}) \\ \mathbf{y} &= \mathbf{x} + \text{Proj}(\text{SoftMax}(\frac{\mathbf{q}\mathbf{k}}{c})\mathbf{v}) \\ \mathbf{z} &= \mathbf{y} + \text{FFN}(\mathbf{y}), \end{aligned}$$

where  $c$  is a constant, Proj represents a projection layer, Emb comprises a layer norm and a projection layer, and FFN stands for a feed-forward network. Finally, the updated class embedding is used to represent the whole image:  $x_{\text{image}} = \mathbf{z}[0]$ <sup>2</sup>.

**CLIP’s Dense Representation.** To extract the dense feature map from a CLIP ViT, we follow (Zhou et al., 2022a) to slightly modify the last residual attention block. Specifically, we keep the projection layers, layer norms, and FFNs while discarding the self-attention. The modified residual attention block  $\mathbf{z}' = \text{ModifiedResAttn}(\mathbf{x})$  can be written as:

$$\begin{aligned} \mathbf{v} &= \text{Emb}_v(\mathbf{x}) \\ \mathbf{y}' &= \mathbf{x} + \text{Proj}(\mathbf{v}) \\ \mathbf{z}' &= \mathbf{y}' + \text{FFN}(\mathbf{y}'). \end{aligned}$$

We discard the class embedding  $\mathbf{z}'[0]$  and reshape the image embeddings  $\mathbf{z}'[1 : h \times w]$  into an  $h \times w$  feature map  $\mathcal{X}_{\text{dense}}$ , from which we can extract representations for boxes or masks by RoIAlign or mask pooling (He et al., 2017).

**Discussion and Motivation of CLIPSelf.** Although the dense features have been used in existing works (Zhou et al., 2022a; Wu et al., 2023b; Cho et al., 2023) to extract box or mask representations for dense prediction tasks, we make the first attempt to provide an in-depth analysis of the dense representation. Specifically, we compare the recognition ability of image representation and dense representation by using them to classify the region boxes annotated in the COCO dataset (Lin et al., 2014). Given an image and a region box annotation, the dense representation of the region can be extracted from  $\mathcal{X}_{\text{dense}}$  by pooling (RoIAlign). For image representation, we crop the region box from the image first and then send it to the CLIP model to obtain  $x_{\text{image}}$ .

<sup>2</sup>Usually, there is a linear output layer following the last attention module. We ignore it for brevity.

Given an image and a region box annotation, the dense representation of the region can be extracted from Xdense by pooling (RoIAlign) it uses 2 stage where regions are extracted and ROI Align is performed. For image representation, we crop the region box from the image first and then send it to the CLIP model to obtain  $x_{image}$ .

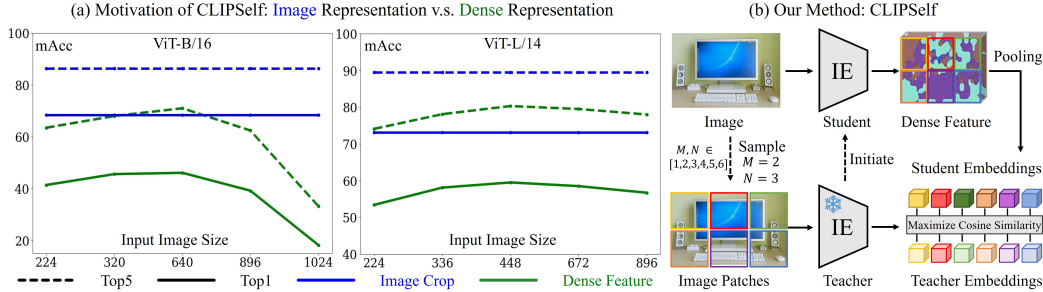


Figure 3: (a) Region classification using image representation (blue) and dense representation (green) of CLIP ViTs. The y-axis stands for the mean accuracy (mAcc). The x-axis is the input image size for obtaining dense feature maps (green). The input size for image representation (blue) of the image crops is fixed at  $224 \times 224$  for ViT-B/16 and  $336 \times 336$  for ViT-L/14. (b) CLIPSelf randomly splits an image into patch regions for self-distillation. Then it aligns the region representation pooled (by RoIAlign) from the dense feature map of the student to the corresponding image representation of the Teacher. **Teacher:** the original CLIP ViT; **Student:** the fine-tuned CLIP ViT.

As shown in Fig. 3, the image representation (blue) outperforms the dense representation (green) on both Top1 and Top5 classification accuracy by a considerable margin across all input sizes. It is noticeable that the performance of ViTs’ dense representation does not grow with the input image size, which hinders the use of the models for downstream tasks like object detection and image segmentation, where large image resolution is always desired. This phenomenon is primarily attributed to the lack of inductive bias in the design of CLIP ViTs, where the vision-language alignment on the representation of the images *cannot* be directly transferred to local regions. Based on the results in Fig. 3(a), we believe the region representations extracted from the dense feature map can be improved by aligning them to the image representations of the corresponding image crops.

### 3.2 CLIPSELF

We propose a simple self-distillation approach, CLIPself, that allows CLIP ViTs to teach themselves by aligning the region representations pooled from dense feature maps to the image representations of the corresponding image crops as shown in Fig. 3(b). We denote the original CLIP model as **Teacher** and the fine-tuned CLIP model as **Student**. The weights of the Teacher are fixed, while the weights of the Student are initialized with the weights of the Teacher. To train the Student, we partition the image into regions and align the Student’s dense representations of the regions to the corresponding image representations of the Teacher.

**Image Patches as Regions.** For self-distillation purposes, we divide an image into a grid of  $m \times n$  patches. During each training iteration,  $m$  and  $n$  are randomly selected from the set  $\{1, \dots, M\}$  to allow different patch sizes. Empirically, we set  $M = 6$  in our implementation. Our experiments found that such a simple patch sampling scheme can already enhance the Student’s dense representation remarkably. Moreover, the grid image patches are more effective in covering background content (referred to as ‘stuff’) than region proposals generated by external models, which predominantly focus on foreground objects (referred to as ‘thing’). This is validated by the results of classifying stuff masks in Tab. 2.

**Self-Distillation.** Given an image, we can obtain the dense feature map  $\mathcal{X}_{dense}$  from the Student as described in Sec. 3.1. Given the  $m \times n$  patch regions, the Student embedding of patch  $\mathcal{P}^{ij}$  ( $i \in \{0, \dots, m-1\}$ ,  $j \in \{0, \dots, n-1\}$ ) can be denoted as  $s_{dense}^{ij} = \text{Pooling}(\mathcal{X}_{dense}, \mathcal{P}^{ij})$ . Correspondingly, the teacher embedding  $t_{image}^{ij}$  is obtained by sending  $\mathcal{P}^{ij}$  to the Teacher for image representation. Consequently, the self-distillation loss to align student and teacher embeddings can be written as:

$$\mathcal{L} = \frac{1}{m \times n} \sum_{i=0}^{m-1} \sum_{j=0}^{n-1} \left( 1 - \frac{s_{dense}^{ij} \cdot t_{image}^{ij}}{|s_{dense}^{ij}| \cdot |t_{image}^{ij}|} \right).$$

Table 1: Ablation study on the design choices of CLIPSelf. The row with blue color is our default choice in the main experiment. The experiments are on ViT-B/16 from EVA-CLIP. #1 in all the sub-tables stands for the original EVA-CLIP ViT. #5\* in (c) stands for the sanity check.

(a) Number of image patches			(b) Number of learnable layers			(c) Input image size of Student		
#	Training Patch Split	Mean Accuracy Top1 Top5	#	Learnable Layers	Mean Accuracy Top1 Top5	#	Input Image Size	Mean Accuracy Top1 Top5
1	-	18.2 33.2	1	-	18.2 33.2	1	-	18.2 33.2
2	M=4	71.3 90.1	2	3	45.0 71.1	2	320	46.5 70.1
3	M=6	72.1 91.3	3	6	59.4 82.3	3	640	67.1 87.7
4	M=8	71.6 91.1	4	9	68.7 88.7	4	1024	72.1 91.3
5	M=10	70.0 90.2	5	12	72.1 91.3	5*	1024	52.3 76.4

### 3.3 APPLICATION TO OPEN-VOCABULARY DENSE PREDICTION

For open-vocabulary object detection, we build a two-stage detector on a frozen CLIP ViT backbone and only train the detection heads following F-VLM (Kuo et al., 2023). And we replace the backbone with the CLIPSelf fine-tuned model. As the detection task primarily targets at foreground objects, we keep using region proposals as an option for implementing CLIPSelf in the context of open-vocabulary object detection. Please refer to the appendix A.3 for the details of the detector. For semantic segmentation, our fine-tuned CLIP ViTs can serve as better initialization for Cat-Seg (Cho et al., 2023). For panoptic segmentation, our fine-tuned ViT can be applied to the inference stage of ODISE (Xu et al., 2023a) to improve open-vocabulary ability.

## 4 EXPERIMENTS

In this part, we first introduce the ablation study of the design choices of CLIPSelf in Sec. 4.1. In Sec. 4.2, we show the enhanced dense representation of our refined CLIP ViTs both qualitatively and quantitatively. Then, we report the benchmark results on open-vocabulary object detection and image segmentation in Sec. 4.3. Lastly, we compare CLIPSelf by using region-text pairs to substantiate further the superiority of CLIPSelf in Sec. 4.4.

### 4.1 ABLATION STUDY OF CLIPSELF

**Experiment Setting.** To train CLIPSelf, we use 8 A100 GPUs and set the batch size as 2 on each GPU. We train the models for 6 epochs using the AdamW (Loshchilov & Hutter, 2017) optimizer with a learning rate of  $1e-5$  and weight decay of 0.1. By default, we use the images in `train2017` split of COCO dataset (Lin et al., 2014), which are exactly the training images of most downstream open-vocabulary benchmarks. All experiments in Sec. 4.1 are conducted on the ViT-B/16 from EVA-CLIP (Sun et al., 2023) considering its high efficiency and capacity, and we assume using image patches for self-distillation unless otherwise stated. The mean accuracy (mAcc) of classifying region boxes annotated in COCO’s `val2017` split is used as the indicator for evaluation.

**Design Choices.** We conduct ablation studies on design choices of CLIPSelf, namely *patch split*, *trainable layers*, and *input size of the Student*. For the *patch split*, an image is split into a grid of  $m \times n$  patches, where  $m$  and  $n$  are randomly sampled from  $\{1, \dots, M\}$ . In Tab. 1a, we show the results when  $M$  is set as 4, 6, and 8. The results support our choice of  $M = 6$  as it achieves the highest accuracy. For the number of *trainable layers*, we experiment with updating the last 3, 6, 9, and 12 attention layers of ViT-B/16. As shown in Tab. 1b, the region classification accuracy consistently improves with more trainable layers. Therefore, we choose to update all the attention modules in our implementation of CLIPSelf. For the *input size of the Student*, we experiment with different input image sizes ( $320 \times 320, 640 \times 640, 1024 \times 1024$ ). The input to the Teacher is fixed at  $224 \times 224$ . As shown in Tab. 1c, training with larger images for the Student improves the performance of region classification. Therefore, we set  $1024 \times 1024$  as the default input size for the Student. However, considering the memory cost, we do not further increase the image size. For the input size and trainable layers on ViT-L/14, please refer to the appendix A.2.

**Sanity Check on Input Image Size.** The aforementioned ablation study on input image size of the Student reveals the efficacy of training with larger inputs, which raises a question on whether the improvement of CLIPSelf is merely contributed to training the Student with higher image resolution

Table 2: Enhancement of dense representation. We report the Top1 and Top5 mean accuracy on classifying boxes and panoptic masks (thing and stuff).

#	Model	Method	Region Proposals	Boxes		Thing Masks		Stuff Masks	
				Top1	Top5	Top1	Top5	Top1	Top5
1	ViT-B/16	-	-	18.2	33.2	20.6	36.5	18.4	43.5
2	ViT-B/16	CLIPSelf	✗	72.1	91.3	74.4	91.8	<b>46.8</b>	<b>80.2</b>
3	ViT-B/16	CLIPSelf	✓	<b>74.0</b>	<b>92.6</b>	<b>76.3</b>	<b>92.8</b>	36.8	75.0

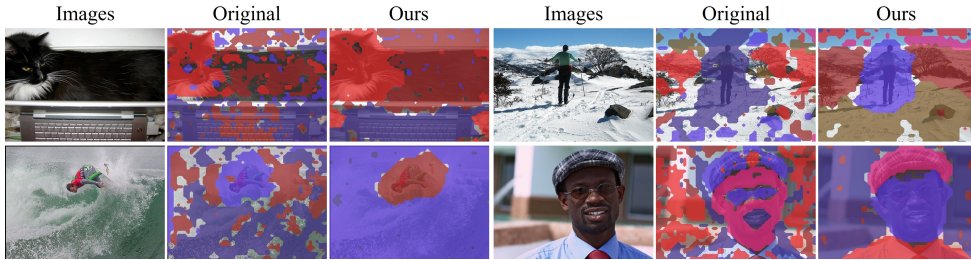


Figure 4: K-Means visualization of the dense feature maps of CLIP ViT. We show the raw images, the K-Means results of the original model, and those of our fine-tuned model by CLIPSelf.

instead of the region-wise supervision in the self-distillation. Therefore, we add a sanity check to assess to what extent the dense representation is enhanced by merely increasing the image size. Specifically, we train the Student with input size  $1024 \times 1024$  using the image-level supervision from COCO Caption dataset (Chen et al., 2015). As shown in Tab. 1c(#5), image-level supervision with large input size only improves the Top1 mAcc to 52.1%, lagging behind the result of our self-distillation approach (72.1%) by a considerable margin.

#### 4.2 ENHANCEMENT OF DENSE REPRESENTATION BY CLIPSELF

**Quantitative Evaluation.** We conduct a comprehensive evaluation on the enhancement of CLIP ViT’s dense representation. In addition to the region box classification introduced in Sec. 4.1, we also report the mAcc of classifying panoptic masks (thing and stuff) annotated in COCO Panoptic dataset (Kirillov et al., 2019b). The mask embeddings for classification are extracted from the dense feature maps of the CLIP ViT by mask pooling (He et al., 2017). As shown in Tab. 2(#1&#2), CLIP-Self not only improves the ViTs’ recognition ability for region boxes but also for panoptic masks, which establishes CLIPSelf as a general solution to both open-vocabulary object detection and open-vocabulary image segmentation. Further results of various ViT variants are in the appendix A.2.

**Using Region Proposals.** We also implement CLIPSelf using region proposals generated by a region proposal network (RPN) trained on COCO `train2017` split. To satisfy the open-vocabulary setting, the RPN is trained solely using annotations of the 48 base object categories defined in OV-COCO. As shown in Tab. 2(#3), leveraging region proposals boosts the classification accuracy for foreground instances, including object boxes and thing masks. However, this approach exhibits reduced proficiency in recognizing background contents (stuff masks) since the training of CLIPSelf has primarily emphasized foreground instances. Consequently, the utilization of region proposals is considered an alternative option only for open-vocabulary object detection.

**Qualitative Results.** We present visualizations of the CLIP ViT’s dense representation by employing K-Means clustering (Lloyd, 1982) on the dense feature maps, where pixels of high cosine similarities are grouped into clusters. For clarity, we discard clusters with only a few pixels. As depicted in Fig. 4, our fine-tuned CLIP ViT demonstrates improved accuracy in gathering pixels belonging to the same object into a single cluster, *e.g.*, the ‘human face’ and the ‘hat’ in the bottom right example. Additionally, our CLIPSelf model exhibits a reduction in false positive clusters, which either cover a small portion of an object or include pixels from different objects. The improved K-Means cluster results serve as visible evidence of the enhancement of the CLIP ViT’s dense representation.

#### 4.3 APPLICATION TO OPEN-VOCABULARY TASKS

**Experiment Setting.** We employ the refined CLIP ViTs to open-vocabulary dense prediction tasks. To ensure a fair comparison on each open-vocabulary benchmark, we implement CLIPSelf using the training set of the corresponding benchmark. Concretely, for open-vocabulary detection on

Table 3: Results on open-vocabulary object detection. † means using learnable category prompt for region classification. \* stands for methods that obtain open-vocabulary ability from both CLIP visual model and additional image annotations (*e.g.*, image captions).

(a) OV-COCO benchmark			(b) OV-LVIS benchmark		
Method	Backbone	AP <sub>50</sub> <sup>novel</sup>	Method	Backbone	mAP <sub>r</sub>
OV-RCNN (Zareian et al., 2021)	RN50	17.5	ViLD (Gu et al., 2021)	RN50	16.6
RegionCLIP (Zhong et al., 2022)	RN50	26.8	OV-DETR (Zang et al., 2022)	RN50	17.4
ViLD (Gu et al., 2021)	RN50	27.6	DetPro (Du et al., 2022) <sup>†</sup>	RN50	19.8
Detic (Zhou et al., 2022b)	RN50	27.8	OC-OVD (Rasheed et al., 2022)*	RN50	21.1
F-VLM (Kuo et al., 2023)	RN50	28.0	OADP (Wang et al., 2023)	RN50	21.7
OV-DETR (Zang et al., 2022)	RN50	29.4	RegionCLIP (Zhong et al., 2022)	RN50x4	22.0
VLDet (Lin et al., 2023)	RN50	32.0	CORA (Wu et al., 2023c) <sup>†</sup>	RN50x4	22.2
RO-ViT (Kim et al., 2023)	ViT-L/16	33.0	BARON-KD (Wu et al., 2023b) <sup>†</sup>	RN50	22.6
BARON-Cap (Wu et al., 2023b)	RN50	33.1	VLDet (Lin et al., 2023)	SwinB	26.3
BARON-KD (Wu et al., 2023b)	RN50	34.0	CORA+ (Wu et al., 2023c) <sup>†*</sup>	RN50x4	28.1
OC-OVD (Rasheed et al., 2022)*	RN50	36.6	F-VLM (Kuo et al., 2023)	RN50x64	32.8
CORA (Wu et al., 2023c) <sup>†</sup>	RN50x4	41.7	Detic (Zhou et al., 2022b)	SwinB	33.8
CORA+ (Wu et al., 2023c) <sup>†*</sup>	RN50x4	43.1	RO-ViT (Kim et al., 2023)	ViT-H/16	34.1
F-ViT	ViT-B/16	17.5	F-ViT	ViT-B/16	11.5
F-ViT+CLIPSelf	ViT-B/16	37.6	F-ViT+CLIPSelf	ViT-B/16	25.3
F-ViT	ViT-L/14	24.7	F-ViT	ViT-L/14	24.2
F-ViT+CLIPSelf	ViT-L/14	<b>44.3</b>	F-ViT+CLIPSelf	ViT-L/14	<b>34.9</b>

Table 4: Transfer evaluation of the LVIS-trained detector on COCO and Objects365 datasets. We use the detector with the ViT-L/14 backbone refined by CLIPSelf. ‡ stands for the results of ViLD (Gu et al., 2021) reproduced in DetPro (Du et al., 2022).

Method	COCO						Objects365					
	AP	AP <sub>50</sub>	AP <sub>75</sub>	AP <sub>s</sub>	AP <sub>m</sub>	AP <sub>l</sub>	AP	AP <sub>50</sub>	AP <sub>75</sub>	AP <sub>s</sub>	AP <sub>m</sub>	AP <sub>l</sub>
ViLD (Gu et al., 2021)	36.6	55.6	39.6	-	-	-	11.8	18.0	12.6	-	-	-
ViLD (Gu et al., 2021) <sup>‡</sup>	34.1	52.3	36.5	21.6	38.9	46.1	11.5	17.8	12.3	4.2	11.1	17.8
DetPro (Du et al., 2022)	34.9	53.8	37.4	22.5	39.6	46.3	12.1	18.8	12.9	4.5	11.5	18.6
BARON (Wu et al., 2023b)	36.2	55.7	39.1	24.8	40.2	47.3	13.6	21.0	14.5	5.0	13.1	20.7
RO-ViT (Kim et al., 2023)	-	-	-	-	-	-	17.1	26.9	19.5	-	-	-
F-VLM (Kuo et al., 2023)	39.8	61.6	43.8	-	-	-	17.7	27.4	19.1	-	-	-
F-ViT+CLIPSelf	<b>40.5</b>	<b>63.8</b>	<b>44.3</b>	<b>26.8</b>	<b>44.6</b>	<b>53.8</b>	<b>19.5</b>	<b>31.3</b>	<b>20.7</b>	<b>9.7</b>	<b>23.2</b>	<b>35.5</b>

OV-COCO benchmark, the `train2017` split of COCO dataset (Lin et al., 2014) is used for self-distillation. For the OV-LVIS benchmark, the images from the `train` split of LVIS v1.0 (Gupta et al., 2019) are used. For open-vocabulary image segmentation tasks, we use the `train2017` split of the COCO dataset for both the semantic and panoptic segmentation benchmarks.

**Open-Vocabulary Object Detection.** Following F-VLM (Kuo et al., 2023), which freezes the CLIP backbone, we introduce a two-stage detector baseline built on frozen CLIP ViTs, called *F-ViT*. To extract multi-scale feature maps from the frozen backbone, we interpolate the feature maps from the intermediate layers of ViTs. We use the ViTs from EVA-CLIP (Sun et al., 2023) for our main experiments for their efficiency and high capacity. To train the detector, we set the batch size to 8 on each GPU and employ the AdamW (Loshchilov & Hutter, 2017) optimizer with a learning rate of  $1e-4$  and weight decay of 0.1. We train the models for 3 epochs on the OV-COCO benchmark and 48 epochs on the OV-LVIS benchmark. For evaluation, we follow previous works to use box AP at IoU 0.50 on novel categories (AP<sub>50</sub><sup>novel</sup>) as the metric on OV-COCO, and the mean mask AP on rare categories (mAP<sub>r</sub>) as the metric on OV-LVIS. The results are shown in Tab. 3a and Tab. 3b. By replacing the frozen CLIP ViTs with CLIPSelf fine-tuned models, the performance of F-ViT is significantly improved (44.3 vs 24.7 AP<sub>50</sub><sup>novel</sup> on OV-COCO and 34.9 vs 24.2 mAP<sub>r</sub> on OV-LVIS) and our CLIPSelf outperforms the existing open-vocabulary object detection methods on the two benchmarks. Additionally, we evaluate the detector (ViT-L/14) trained on OV-LVIS on the validation split of COCO (Lin et al., 2014) and Objects365 v1 (Shao et al., 2019) datasets. Our approach consistently outperforms all previous methods in the transfer evaluation. More details on open-vocabulary object detection are in the appendix A.3.

**Open-Vocabulary Semantic Segmentation.** We apply CLIPSelf fine-tuned models to Cat-Seg (Cho et al., 2023), where the dense features of CLIP ViTs (ViT-B/16 and ViT-L/14 from OpenAI) are used in a cost-aggregation module. The segmentation model is trained on COCO Stuff (Caesar et al., 2018) and evaluated on ADE20K (Zhou et al., 2017) (ADE-150 and ADE-847) and PASCAL Context (Mottaghi et al., 2014) datasets using mean Intersection over Union (mIoU)

Table 5: Results on open-vocabulary semantic segmentation.

Method	Model	ADE-150		ADE-847		PASCAL Context	
		mIoU	mAcc	mIoU	mAcc	mIoU	mAcc
OVSeg (Liang et al., 2023)	ViT-B/16	24.8	-	7.1	-	53.3	-
MaskCLIP (Ding et al., 2023)	ViT-L/14	23.7	-	8.2	-	45.9	-
SAN (Xu et al., 2023b)	ViT-B/16	27.5	45.6	10.1	21.1	53.8	73.0
SAN (Xu et al., 2023b)	ViT-L/14	32.1	50.7	<b>12.4</b>	25.2	57.7	77.6
Cat-Seg (Cho et al., 2023)	ViT-B/16	27.2	41.2	8.4	16.6	57.5	74.0
Cat-Seg (Cho et al., 2023)	ViT-L/14	31.5	46.2	10.8	20.5	62.0	78.3
Cat-Seg+CLIPSelf	ViT-B/16	29.0	46.0	9.3	20.1	58.0	75.3
Cat-Seg+CLIPSelf	ViT-L/14	<b>34.5</b>	<b>54.8</b>	<b>12.4</b>	<b>25.4</b>	<b>62.3</b>	<b>80.7</b>

Table 6: Results on open-vocabulary panoptic segmentation. † means the results are obtained by running ODISE’s officially released code and model.

Method	Model	Score		COCO Panoptic			ADE20K		
		CLIP	Pred	PQ	mAP	mIoU	PQ	mAP	mIoU
MaskCLIP (Ding et al., 2023)	ViT-L/14	-	-	-	-	-	15.1	6.0	23.7
ODISE (Xu et al., 2023a)†	ViT-L/14	✓	✗	27.6	26.2	23.7	15.3	9.8	17.3
ODISE (Xu et al., 2023a)†	ViT-L/14	✓	✓	45.3	38.1	<b>52.3</b>	22.9	13.4	28.5
ODISE+CLIPSelf	ViT-L/14	✓	✗	35.1	30.9	36.7	19.5	10.6	24.5
ODISE+CLIPSelf	ViT-L/14	✓	✓	<b>45.7</b>	<b>38.5</b>	<b>52.3</b>	<b>23.7</b>	<b>13.6</b>	<b>30.1</b>

Table 7: Comparison with using region-text pairs. We report the Top1 and Top5 mAcc of classifying boxes and panoptic masks. We also report the APs on OV-COCO in the rightmost two columns.

#	Model	Method	Region Proposals	Boxes		Thing Masks		Stuff Masks		OV-COCO	
				Top1	Top5	Top1	Top5	Top1	Top5	AP <sub>50</sub> <sup>novel</sup>	AP <sub>50</sub>
1	ViT-B/16	Region-Text	✓	71.1	90.7	73.7	91.4	34.2	68.6	34.4	49.0
2	ViT-B/16	CLIPSelf	✓	<b>74.0</b>	<b>92.6</b>	<b>76.3</b>	<b>92.8</b>	<b>36.8</b>	<b>75.0</b>	<b>37.6</b>	<b>50.4</b>

and mean pixel accuracy (mAcc) as the main metrics. As shown in Tab. 5, CLIPSelf leads to performance improvement across all the test datasets. Notably, there is a significant increase in mAcc, indicating enhanced per-pixel classification performance.

**Open-Vocabulary Panoptic Segmentation.** We first reproduce ODISE (Xu et al., 2023a) using the original CLIP model (ViT-L/14 from OpenAI) by running its officially released model and code<sup>3</sup>. Subsequently, we apply our fine-tuned model during the inference stage of ODISE, where the CLIP score and the score predicted by the mask generator are fused to classify the panoptic masks. The model is trained on the COCO Panoptic (Lin et al., 2014) dataset and evaluated on ADE20K (Zhou et al., 2017) dataset. Panoptic quality (PQ) (Kirillov et al., 2019a) is the main metric. We also use mAP and mIoU for evaluation. Tab. 6 presents the results of using the CLIP score only and using the fused score. The observed improvements in Tab. 6 indicate the enhanced recognition capability of ViT’s dense representation for recognizing panoptic masks.

#### 4.4 COMPARISON WITH USING REGION-TEXT PAIRS

To further evaluate the effectiveness of CLIPSelf, we compare it with the method using region-text pairs. We follow the principle of RegionCLIP (Zhong et al., 2022) that matches region proposals with object nouns to generate region-text pairs. For a fair comparison, CLIPSelf also employs region proposals. Further details regarding the refinement of CLIP ViTs using region-text pairs are provided in the appendix A.4. As indicated in Tab. 7(#1&#2), CLIPSelf outperforms the method using noisy region-text pairs by a large margin when implemented in fair conditions.

## 5 CONCLUSION

In this paper, we undertake a comprehensive analysis of the dense representation of ViT-based CLIP models, which is essential for downstream dense prediction tasks. Based on this analysis, we introduce CLIPSelf, which fine-tunes CLIP ViTs’ dense representation through self-distillation. Our approach does not rely on expensive region-text pairs. Instead, it leverages CLIP’s image representation on image patches to improve CLIP’s dense representation without the need for manual

<sup>3</sup><https://github.com/NVlabs/ODISE>

annotation. The fine-tuned CLIP ViTs significantly surpass the performance of the original models when applied to open-vocabulary object detection and image segmentation. In conclusion, our CLIPSelf serves as a straightforward yet effective solution to enhance the dense representation of CLIP ViTs, which is critical to open-vocabulary dense prediction tasks.

## REFERENCES

- Holger Caesar, Jasper Uijlings, and Vittorio Ferrari. Coco-stuff: Thing and stuff classes in context. In *IEEE Conf. Comput. Vis. Pattern Recog.*, 2018.
- Xinlei Chen, Hao Fang, Tsung-Yi Lin, Ramakrishna Vedantam, Saurabh Gupta, Piotr Dollár, and C Lawrence Zitnick. Microsoft coco captions: Data collection and evaluation server. *arXiv preprint arXiv:1504.00325*, 2015.
- Seokju Cho, Heeseong Shin, Sunghwan Hong, Seungjun An, Seungjun Lee, Anurag Arnab, Paul Hongsuck Seo, and Seunghyong Kim. Cat-seg: Cost aggregation for open-vocabulary semantic segmentation. *arXiv preprint arXiv:2303.11797*, 2023.
- Jian Ding, Nan Xue, Gui-Song Xia, and Dengxin Dai. Decoupling zero-shot semantic segmentation. In *IEEE Conf. Comput. Vis. Pattern Recog.*, pp. 11583–11592, 2022.
- Zheng Ding, Jieke Wang, and Zhuowen Tu. Open-vocabulary universal image segmentation with maskclip. In *ICML*, 2023.
- Yu Du, Fangyun Wei, Zihe Zhang, Miaojing Shi, Yue Gao, and Guoqi Li. Learning to prompt for open-vocabulary object detection with vision-language model. In *IEEE Conf. Comput. Vis. Pattern Recog.*, 2022.
- Andrea Frome, Greg S Corrado, Jon Shlens, Samy Bengio, Jeff Dean, Marc’Aurelio Ranzato, and Tomas Mikolov. Devise: A deep visual-semantic embedding model. *Adv. Neural Inform. Process. Syst.*, 2013.
- Mingfei Gao, Chen Xing, Juan Carlos Niebles, Junnan Li, Ran Xu, Wenhao Liu, and Caiming Xiong. Open vocabulary object detection with pseudo bounding-box labels. In *Eur. Conf. Comput. Vis.*, 2022.
- Golnaz Ghiasi, Xiuye Gu, Yin Cui, and Tsung-Yi Lin. Open-vocabulary image segmentation. *arXiv preprint arXiv:2112.12143*, 2021.
- Ross Girshick. Fast r-cnn. In *Int. Conf. Comput. Vis.*, 2015.
- Xiuye Gu, Tsung-Yi Lin, Weicheng Kuo, and Yin Cui. Open-vocabulary object detection via vision and language knowledge distillation. In *Int. Conf. Learn. Represent.*, 2021.
- Agrim Gupta, Piotr Dollár, and Ross B. Girshick. LVIS: A dataset for large vocabulary instance segmentation. In *IEEE Conf. Comput. Vis. Pattern Recog.*, 2019.
- Tanmay Gupta, Arash Vahdat, Gal Chechik, Xiaodong Yang, Jan Kautz, and Derek Hoiem. Contrastive learning for weakly supervised phrase grounding. In *Eur. Conf. Comput. Vis.*, 2020.
- Bharath Hariharan, Pablo Arbeláez, Ross Girshick, and Jitendra Malik. Simultaneous detection and segmentation. In *Eur. Conf. Comput. Vis.*, 2014.
- Kaiming He, Georgia Gkioxari, Piotr Dollár, and Ross Girshick. Mask R-CNN. In *Int. Conf. Comput. Vis.*, 2017.
- Dinesh Jayaraman and Kristen Grauman. Zero-shot recognition with unreliable attributes. In *Adv. Neural Inform. Process. Syst.*, 2014.
- Chao Jia, Yinfai Yang, Ye Xia, Yi-Ting Chen, Zarana Parekh, Hieu Pham, Quoc Le, Yun-Hsuan Sung, Zhen Li, and Tom Duerig. Scaling up visual and vision-language representation learning with noisy text supervision. In *ICML*, 2021.

- Dahun Kim, Anelia Angelova, and Weicheng Kuo. Region-aware pretraining for open-vocabulary object detection with vision transformers. In *IEEE Conf. Comput. Vis. Pattern Recog.*, 2023.
- Wonjae Kim, Bokyung Son, and Ildoo Kim. ViLT: Vision-and-language transformer without convolution or region supervision. In *ICML*, 2021.
- Alexander Kirillov, Kaiming He, Ross Girshick, Carsten Rother, and Piotr Dollár. Panoptic segmentation. In *IEEE Conf. Comput. Vis. Pattern Recog.*, pp. 9404–9413, 2019a.
- Alexander Kirillov, Kaiming He, Ross B. Girshick, Carsten Rother, and Piotr Dollár. Panoptic segmentation. *IEEE Conf. Comput. Vis. Pattern Recog.*, 2019b.
- Ranjay Krishna, Yuke Zhu, Oliver Groth, Justin Johnson, Kenji Hata, Joshua Kravitz, Stephanie Chen, Yannis Kalantidis, Li-Jia Li, David A Shamma, et al. Visual genome: Connecting language and vision using crowdsourced dense image annotations. *Int. J. Comput. Vis.*, 2017.
- Weicheng Kuo, Yin Cui, Xiuye Gu, A. J. Piergiovanni, and Anelia Angelova. F-VLM: Open-vocabulary object detection upon frozen vision and language models. *Int. Conf. Learn. Represent.*, 2023.
- Liunian Harold Li, Pengchuan Zhang, Haotian Zhang, Jianwei Yang, Chunyuan Li, Yiwu Zhong, Lijuan Wang, Lu Yuan, Lei Zhang, Jenq-Neng Hwang, Kai-Wei Chang, and Jianfeng Gao. Grounded language-image pre-training. In *IEEE Conf. Comput. Vis. Pattern Recog.*, 2022a.
- Yanghao Li, Hanzi Mao, Ross Girshick, and Kaiming He. Exploring plain vision transformer backbones for object detection. In *Eur. Conf. Comput. Vis.*, 2022b.
- Feng Liang, Bichen Wu, Xiaoliang Dai, Kunpeng Li, Yinan Zhao, Hang Zhang, Peizhao Zhang, Peter Vajda, and Diana Marculescu. Open-vocabulary semantic segmentation with mask-adapted clip. In *IEEE Conf. Comput. Vis. Pattern Recog.*, 2023.
- Chuang Lin, Peize Sun, Yi Jiang, Ping Luo, Lizhen Qu, Gholamreza Haffari, Zehuan Yuan, and Jianfei Cai. Learning object-language alignments for open-vocabulary object detection. In *ICLR*, 2023.
- Tsung-Yi Lin, Michael Maire, Serge Belongie, James Hays, Pietro Perona, Deva Ramanan, Piotr Dollár, and C Lawrence Zitnick. Microsoft COCO: Common objects in context. In *Eur. Conf. Comput. Vis.*, 2014.
- Shilong Liu, Zhaoyang Zeng, Tianhe Ren, Feng Li, Hao Zhang, Jie Yang, Chunyuan Li, Jianwei Yang, Hang Su, Jun Zhu, et al. Grounding dino: Marrying dino with grounded pre-training for open-set object detection. *arXiv preprint arXiv:2303.05499*, 2023.
- Stuart Lloyd. Least squares quantization in pcm. *IEEE transactions on information theory*, 28(2): 129–137, 1982.
- Ilya Loshchilov and Frank Hutter. Decoupled weight decay regularization. *arXiv preprint arXiv:1711.05101*, 2017.
- Roozbeh Mottaghi, Xianjie Chen, Xiaobai Liu, Nam-Gyu Cho, Seong-Whan Lee, Sanja Fidler, Raquel Urtasun, and Alan Yuille. The role of context for object detection and semantic segmentation in the wild. In *IEEE Conf. Comput. Vis. Pattern Recog.*, pp. 891–898, 2014.
- Jishnu Mukhoti, Tsung-Yu Lin, Omid Poursaeed, Rui Wang, Ashish Shah, Philip HS Torr, and Ser-Nam Lim. Open vocabulary semantic segmentation with patch aligned contrastive learning. In *IEEE Conf. Comput. Vis. Pattern Recog.*, 2023.
- Bryan A Plummer, Liwei Wang, Chris M Cervantes, Juan C Caicedo, Julia Hockenmaier, and Svetlana Lazebnik. Flickr30k entities: Collecting region-to-phrase correspondences for richer image-to-sentence models. In *Int. Conf. Comput. Vis.*, 2015.
- Alec Radford, Jong Wook Kim, Chris Hallacy, Aditya Ramesh, Gabriel Goh, Sandhini Agarwal, Girish Sastry, Amanda Askell, Pamela Mishkin, Jack Clark, et al. Learning transferable visual models from natural language supervision. In *ICML*, 2021.

- Hanoona Rasheed, Muhammad Maaz, Muhammad Uzair Khattak, Salman Khan, and Fahad Shah-baz Khan. Bridging the gap between object and image-level representations for open-vocabulary detection. In *NeurIPS*, 2022.
- Shaoqing Ren, Kaiming He, Ross Girshick, and Jian Sun. Faster r-cnn: Towards real-time object detection with region proposal networks. *Adv. Neural Inform. Process. Syst.*, 28, 2015.
- Robin Rombach, Andreas Blattmann, Dominik Lorenz, Patrick Esser, and Björn Ommer. High-resolution image synthesis with latent diffusion models. In *IEEE Conf. Comput. Vis. Pattern Recog.*, 2022.
- Shuai Shao, Zeming Li, Tianyuan Zhang, Chao Peng, Gang Yu, Xiangyu Zhang, Jing Li, and Jian Sun. Objects365: A large-scale, high-quality dataset for object detection. In *Int. Conf. Comput. Vis.*, 2019.
- Quan Sun, Yuxin Fang, Ledell Wu, Xinlong Wang, and Yue Cao. Eva-clip: Improved training techniques for clip at scale. *arXiv preprint arXiv:2303.15389*, 2023.
- Luting Wang, Yi Liu, Penghui Du, Zihan Ding, Yue Liao, Qiaosong Qi, Biaolong Chen, and Si Liu. Object-aware distillation pyramid for open-vocabulary object detection. In *IEEE Conf. Comput. Vis. Pattern Recog.*, 2023.
- Jianzong Wu, Xiangtai Li, Shilin Xu, Haobo Yuan, Henghui Ding, Yibo Yang, Xia Li, Jiangning Zhang, Yunhai Tong, Xudong Jiang, Bernard Ghanem, and Dacheng Tao. Towards open vocabulary learning: A survey. *arXiv preprint arXiv:2306.15880*, 2023a.
- Size Wu, Wenwei Zhang, Sheng Jin, Wentao Liu, and Chen Change Loy. Aligning bag of regions for open-vocabulary object detection. In *IEEE Conf. Comput. Vis. Pattern Recog.*, 2023b.
- Xiaoshi Wu, Feng Zhu, Rui Zhao, and Hongsheng Li. Cora: Adapting clip for open-vocabulary detection with region prompting and anchor pre-matching. In *IEEE Conf. Comput. Vis. Pattern Recog.*, 2023c.
- Jiarui Xu, Sifei Liu, Arash Vahdat, Wonmin Byeon, Xiaolong Wang, and Shalini De Mello. Open-vocabulary panoptic segmentation with text-to-image diffusion models. In *IEEE Conf. Comput. Vis. Pattern Recog.*, 2023a.
- Mengde Xu, Zheng Zhang, Fangyun Wei, Yutong Lin, Yue Cao, Han Hu, and Xiang Bai. A simple baseline for open-vocabulary semantic segmentation with pre-trained vision-language model. In *Eur. Conf. Comput. Vis.*, 2022.
- Mengde Xu, Zheng Zhang, Fangyun Wei, Han Hu, and Xiang Bai. Side adapter network for open-vocabulary semantic segmentation. *IEEE Conf. Comput. Vis. Pattern Recog.*, 2023b.
- Shilin Xu Xu, Xiangtai Li, Size Wu, Wenwei Zhang, Yining Li, Guangliang Cheng, Yunhai Tong, Kai Chen, and Chen Change Loy. Dst-det: Simple dynamic self-training for open-vocabulary object detection. *arXiv pre-print*, 2023c.
- Yuhang Zang, Wei Li, Kaiyang Zhou, Chen Huang, and Chen Change Loy. Open-vocabulary DETR with conditional matching. *Eur. Conf. Comput. Vis.*, 2022.
- Alireza Zareian, Kevin Dela Rosa, Derek Hao Hu, and Shih-Fu Chang. Open-vocabulary object detection using captions. In *IEEE Conf. Comput. Vis. Pattern Recog.*, 2021.
- Xiaohua Zhai, Xiao Wang, Basil Mustafa, Andreas Steiner, Daniel Keysers, Alexander Kolesnikov, and Lucas Beyer. LiT: Zero-shot transfer with locked-image text tuning. In *IEEE Conf. Comput. Vis. Pattern Recog.*, 2022.
- Haotian Zhang, Pengchuan Zhang, Xiaowei Hu, Yen-Chun Chen, Liunian Li, Xiyang Dai, Lijuan Wang, Lu Yuan, Jenq-Neng Hwang, and Jianfeng Gao. Glipv2: Unifying localization and vision-language understanding. *Adv. Neural Inform. Process. Syst.*, 2022.
- Yiwu Zhong, Jianwei Yang, Pengchuan Zhang, Chunyuan Li, Noel Codella, Liunian Harold Li, Luowei Zhou, Xiyang Dai, Lu Yuan, Yin Li, et al. RegionCLIP: Region-based language-image pretraining. In *IEEE Conf. Comput. Vis. Pattern Recog.*, 2022.

- Bolei Zhou, Hang Zhao, Xavier Puig, Sanja Fidler, Adela Barriuso, and Antonio Torralba. Scene parsing through ade20k dataset. In *IEEE Conf. Comput. Vis. Pattern Recog.*, pp. 633–641, 2017.
- Chong Zhou, Chen Change Loy, and Bo Dai. Extract free dense labels from CLIP. In *Eur. Conf. Comput. Vis.*, 2022a.
- Xingyi Zhou, Rohit Girdhar, Armand Joulin, Phillip Krähenbühl, and Ishan Misra. Detecting twenty-thousand classes using image-level supervision. In *Eur. Conf. Comput. Vis.*, 2022b.
- Xueyan Zou, Zi-Yi Dou, Jianwei Yang, Zhe Gan, Linjie Li, Chunyuan Li, Xiyang Dai, Harkirat Behl, Jianfeng Wang, Lu Yuan, et al. Generalized decoding for pixel, image, and language. In *IEEE Conf. Comput. Vis. Pattern Recog.*, 2023.

## A APPENDIX

### A.1 CLIP MODELS’ DENSE REPRESENTATION

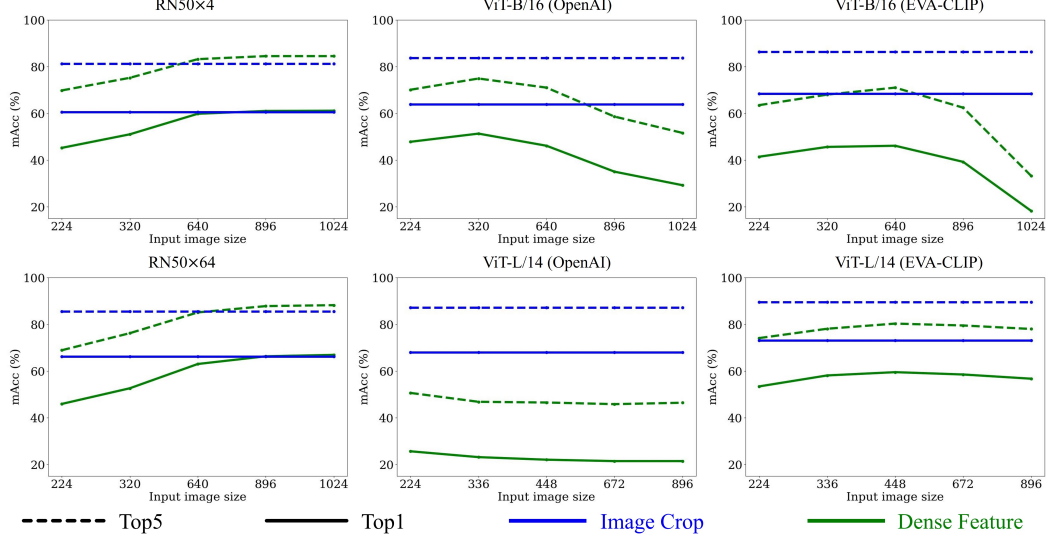


Figure A1: Region classification using CLIP Models. The x-axis of the figures stands for the input size to obtain dense features. The input size for the image-level representation of the image crops is fixed at  $288 \times 288$  for RN50 $\times 4$ ,  $448 \times 448$  for RN50 $\times 64$ ,  $224 \times 224$  for ViT-B/16 and  $336 \times 336$  for ViT-L/14.

Table A1: Different extraction methods to obtain dense features.

#	Model	Source	Method	Boxes Top1	Boxes Top5	Thing Masks Top1	Thing Masks Top5	Stuff Masks Top1	Stuff Masks Top5
1	ViT-B/16	OpenAI	Image Crops	63.8	83.7	-	-	-	-
2	ViT-B/16	OpenAI	(Zhou et al., 2022a)	29.3	51.6	33.5	56.0	25.9	50.9
3	ViT-B/16	OpenAI	Masked Attention	28.2	46.7	29.6	47.5	32.2	61.6
4	ViT-B/16	OpenAI	CLIPSelf	67.4	88.4	69.4	88.5	43.4	76.9

**Region Recognition.** We conduct a comprehensive analysis of the dense representation of CLIP models in the context of region recognition. Specifically, we evaluate the Top1 and Top5 mean accuracy (mAcc) of region classification using the dense features of CLIP models with varying input image sizes. Fig. A1 illustrates the results obtained. For CNN-based models, we observe that their dense features are highly effective for region recognition. In fact, the performance of region recognition using dense feature maps surpasses that of utilizing image-level representations of the corresponding image crops, particularly when the input image size exceeds  $640 \times 640$ . The remarkable alignment between regions and language exhibited by CLIP CNNs enables their straightforward application to downstream open-vocabulary dense prediction tasks. However, the trend is opposite for CLIP Vision Transformers (ViTs). The dense features of ViTs exhibit inferior performance in region classification across all input image sizes. Moreover, the accuracy tends to decrease as the input image size is further increased. Meanwhile, employing ViTs’ image-level representation of the regions’ image crops yields satisfactory results, indicating that it can serve as a reliable teacher for refining the dense representation. These findings shed light on the contrasting behaviors of CLIP CNNs and ViTs, emphasizing the potential benefits of leveraging image-level representations to refine the dense representation of ViTs.

**Dense Feature Extraction.** We follow the practice in (Zhou et al., 2022a) to extract dense feature maps of CLIP ViTs. One might question whether applying a masked-attention operation could be a better cure for the inferior dense-level representation. However, as presented in Tab. A1(#3), our experiments indicate that such an approach improves the recognition of stuff masks but worsens the

Table A2: The enhanced dense representations for recognizing boxes, thing masks, and stuff masks.

Model	Source	CLIPSelf	Boxes		Thing Masks		Stuff Masks	
			Top1	Top5	Top1	Top5	Top1	Top5
ViT-B/16	OpenAI	✗	29.3	51.6	33.5	56.0	25.9	50.9
ViT-B/16	OpenAI	✓	67.4	88.4	69.4	88.5	43.4	76.9
ViT-B/16	EVA-CLIP	✗	18.2	33.2	20.6	36.5	18.4	43.5
ViT-B/16	EVA-CLIP	✓	72.1	91.3	74.4	91.8	46.8	80.2
ViT-L/14	OpenAI	✗	21.4	45.9	28.3	52.0	11.8	27.9
ViT-L/14	OpenAI	✓	68.9	89.6	70.0	88.0	35.5	71.5
ViT-L/14	EVA-CLIP	✗	56.7	78.0	59.0	79.8	20.8	41.9
ViT-L/14	EVA-CLIP	✓	77.1	93.3	78.7	93.7	44.4	78.3

Table A3: Design choices of the open-vocabulary object detector. The ‘Backbone LR’ represents the scalar multiplied by the base learning rate (1e-4) in training. ‘Inter’ means using outputs of ViTs’ intermediate layers.

#	Model	FPN	Layers	Backbone LR	AP <sub>50</sub> <sup>novel</sup>	AP <sub>50</sub> <sup>base</sup>	AP <sub>50</sub>
1	ViT-B/16	SimpleFPN	Last	×0.0	23.1	46.6	40.4
2	ViT-B/16	Standard	Last	×0.0	26.5	47.0	41.6
3	ViT-B/16	Standard	Inter	×0.0	<b>33.6</b>	54.2	<b>48.8</b>
4	ViT-B/16	Standard	Inter	×0.01	31.1	56.6	49.9
5	ViT-B/16	Standard	Inter	×0.1	21.8	58.6	48.8

Table A4: Results of OpenAI models on OV-COCO and OV-LVIS benchmarks.

Method	Model	OV-COCO			OV-LVIS			
		AP <sub>50</sub> <sup>novel</sup>	AP <sub>50</sub> <sup>base</sup>	AP <sub>50</sub>	mAP <sub>r</sub>	mAP <sub>c</sub>	mAP <sub>f</sub>	mAP
F-ViT	ViT-B/16	16.0	36.9	31.4	8.3	11.4	19.7	14.1
F-ViT+CLIPSelf	ViT-B/16	29.8	46.9	42.5	21.6	16.2	23.8	20.1
F-ViT	ViT-L/14	9.2	44.3	35.2	10.7	19.6	26.3	20.7
F-ViT+CLIPSelf	ViT-L/14	31.3	49.2	44.6	24.4	21.1	27.5	24.2

classification of object boxes and thing masks. Furthermore, the accuracy improvement for stuff masks achieved through the masked-attention operation lags significantly behind the performance of CLIPSelf (#4).

## A.2 CLIPSELF

**Input Image Sizes & Trainable Layers.** For the Student model, which extracts dense representations, we set the image size of input images as  $1024 \times 1024$  for ViT-B/16 and  $896 \times 896$  for ViT-L/14. As for the Teacher model, which takes cropped image patches as input, we set the input size as  $224 \times 224$  for ViT-B/16 and  $336 \times 336$  for ViT-L/14. In the training of CLIPSelf, we update the 12 attention layers of ViT-B/16 and the 24 attention layers of ViT-L/14.

**Enhancement of Dense Representation.** To summarize the improvements achieved by CLIPSelf in the context of classifying boxes and masks, we provide a summary in Tab. A2. The results clearly demonstrate that CLIPSelf effectively enhances the dense representation of all variants of ViTs.

## A.3 OPEN-VOCABULARY OBJECT DETECTION

**Benchmark Details.** The open-vocabulary COCO (OV-COCO) benchmark, proposed in OV-RCNN (Zareian et al., 2021), splits 65 object categories in COCO dataset (Lin et al., 2014) into 48 base categories and 17 novel categories. The open-vocabulary LVIS (OV-LVIS) benchmark, proposed in ViLD (Gu et al., 2021), sets the 337 rare categories in LVIS v1.0 (Gupta et al., 2019) dataset as novel categories.

**Input Image Size.** In the main experiments using ViTs from EVA-CLIP (Sun et al., 2023), the input image size is set as  $896 \times 896$  for ViT-L/14. For ViT-B/16, the input image size is  $640 \times 640$  on OV-COCO and  $1024 \times 1024$  on OV-LVIS.

Table A5: Detailed comparison on OV-COCO benchmark. † means using learnable category prompts for region classification. \* stands for methods that obtain open-vocabulary ability from both CLIP visual model and additional image annotations (*e.g.*, image captions).

Method	Backbone	AP <sub>50</sub> <sup>novel</sup>	AP <sub>50</sub> <sup>base</sup>	AP <sub>50</sub>
OV-RCNN (Zareian et al., 2021)	RN50	17.5	41.0	34.9
RegionCLIP (Zhong et al., 2022)	RN50	26.8	54.8	47.5
RegionCLIP (Zhong et al., 2022)	RN50	31.4	57.1	50.4
RegionCLIP (Zhong et al., 2022)	RN50x4	39.3	61.6	55.7
ViLD (Gu et al., 2021)	RN50	27.6	59.5	51.2
OV-DETR (Zang et al., 2022)	RN50	29.4	61.0	52.7
PB-OVD (Gao et al., 2022)	RN50	30.8	46.1	42.1
Detic (Zhou et al., 2022b)	RN50	27.8	51.1	45.0
OC-OVD (Rasheed et al., 2022)*	RN50	36.6	54.0	49.4
VLDet (Lin et al., 2023)	RN50	32.0	50.6	45.8
F-VLM (Kuo et al., 2023)	RN50	28.0	-	39.6
BARON-Cap (Wu et al., 2023b)	RN50	33.1	54.8	49.1
BARON-KD (Wu et al., 2023b)	RN50	34.0	60.4	53.5
BARON-Cap&KD (Wu et al., 2023b)*	RN50	42.7	54.9	51.7
OADP (Wang et al., 2023)	RN50	35.6	55.8	50.5
RO-ViT (Kim et al., 2023)	ViT-B/16	30.2	-	41.5
RO-ViT (Kim et al., 2023)	ViT-L/16	33.0	-	47.7
CORA (Wu et al., 2023c)†	RN50	35.1	35.5	35.4
CORA (Wu et al., 2023c)†	RN50x4	41.7	44.5	43.8
CORA+ (Wu et al., 2023c)†*	RN50x4	43.1	60.9	56.2
F-ViT	ViT-B/16	17.5	41.0	34.9
F-ViT+Region-Text	ViT-B/16	34.4	54.2	49.0
F-ViT+CLIPSelf (Image Patch)	ViT-B/16	33.6	54.2	48.8
F-ViT+CLIPSelf (Region Proposal)	ViT-B/16	37.6	54.9	50.4
F-ViT	ViT-L/14	24.7	53.6	46.0
F-ViT+Region-Text	ViT-L/14	38.7	59.6	54.1
F-ViT+CLIPSelf (Image Patch)	ViT-L/14	38.4	60.6	54.8
F-ViT+CLIPSelf (Region Proposal)	ViT-L/14	<b>44.3</b>	64.1	59.0

**F-ViT Architecture.** In this section, we examine the design choices of the baseline open-vocabulary detector, F-ViT. To build an object detector based on ViTs, a popular approach is ViTDet (Li et al., 2022b), which utilizes a simple Feature Pyramid Network (FPN) and only employs feature maps from the last attention layer. The design of ViTDet is based on two observations: (1) the high capacity of ViT allows it to learn detection-related features without additional parameters except a standard FPN, and (2) the output of the last attention layer is trained to provide task-specific representations for object detection. However, in the course of adapting CLIP ViTs for open-vocabulary object detection where we would like to freeze the backbone to retain the vision-language alignment of CLIP (Kuo et al., 2023), these two presuppositions no longer hold since we do not update the ViT to learn the task-specific features. As shown in Tab. A3, using the ViTDet-like architecture (#1) yields the worst results. Transitioning to a standard FPN (#2) slightly improves the performance. Then, we utilize the feature maps from multiple intermediate layers of the ViT (#3) instead of solely relying on the output of the last layer. This design significantly enhances performance for both novel and base categories. Specifically, we interpolate the feature maps from layers [3, 5, 7, 11] of ViT-B/16 with relative scales  $[\frac{1}{4}, \frac{1}{8}, \frac{1}{16}, \frac{1}{32}]$  to the input image size. For ViT-L/14, we interpolate the feature maps from layers [6, 10, 14, 23] with relative scales  $[\frac{1}{3.5}, \frac{1}{7}, \frac{1}{14}, \frac{1}{28}]$  to the input image size.

**Unfreeze the Backbone.** We explore the possibility of updating the parameters of the ViT backbone in our approach. Tab. A3 (#4&#5) presents the impact on performance when gradually increasing the learning rate of the backbone. Notably, while the AP50 for base categories improves, the performance for novel categories decreases. Based on these observations, we opt to maintain a fixed ViT backbone, as the frozen architecture already achieves satisfactory results on base categories.

**OVD results with OpenAI models.** In the main experiments of open-vocabulary detection, we employ ViTs from EVA-CLIP (Sun et al., 2023), given their favorable performance and high efficiency. However, it is worth noting that CLIPSelf can also be applied for other ViT variants. We report the results using ViTs from OpenAI (Radford et al., 2021) in Tab. A4. The input size is  $640 \times 640$  for

Table A6: Detailed comparison on OV-LVIS benchmark. † means using a learnable category prompt for region classification. \* stands for methods that obtain open-vocabulary ability from both CLIP visual model and additional image annotations (*e.g.*, image captions).

Method	Backbone	mAP <sub>r</sub>	mAP <sub>c</sub>	mAP <sub>f</sub>	mAP
RegionCLIP (Zhong et al., 2022)	RN50	17.1	27.4	34.0	28.2
RegionCLIP (Zhong et al., 2022)	RN50x4	22.0	32.1	36.9	32.3
Detic (Zhou et al., 2022b)	RN50	24.9	-	-	32.4
Detic (Zhou et al., 2022b)	SwinB	33.8	-	-	47.0
VLDet (Lin et al., 2023)	RN50	21.7	29.8	34.3	30.1
VLDet (Lin et al., 2023)	SwinB	26.3	39.4	41.9	38.1
ViLD (Gu et al., 2021)	RN50	16.6	24.6	30.3	25.5
OV-DETR (Zang et al., 2022)	RN50	17.4	25.0	32.5	26.6
DetPro (Du et al., 2022)†	RN50	19.8	25.6	28.9	25.9
BARON-KD (Wu et al., 2023b)†	RN50	22.6	27.6	29.8	27.6
OADP (Wang et al., 2023)	RN50	21.7	26.3	29.0	26.6
OC-OVD (Rasheed et al., 2022)*	RN50	21.1	25.0	29.1	25.9
F-VLM (Kuo et al., 2023)	RN50	18.6	-	-	24.2
F-VLM (Kuo et al., 2023)	RN50x4	26.3	-	-	28.5
F-VLM (Kuo et al., 2023)	RN50x16	30.4	-	-	32.1
F-VLM (Kuo et al., 2023)	RN50x64	32.8	-	-	34.9
RO-ViT (Kim et al., 2023)	ViT-B/16	28.0	-	-	30.2
RO-ViT (Kim et al., 2023)	ViT-L/16	32.1	-	-	34.0
RO-ViT (Kim et al., 2023)	ViT-H/16	34.1	-	-	35.1
CORA (Wu et al., 2023c)†	RN50x4	22.2	-	-	-
CORA+ (Wu et al., 2023c)†*	RN50x4	28.1	-	-	-
F-ViT	ViT-B/16	11.5	12.3	20.6	15.4
F-ViT+CLIPSelf (Image Patch)	ViT-B/16	25.3	21.8	29.1	25.2
F-ViT	ViT-L/14	24.2	27.9	31.5	28.7
F-ViT+CLIPSelf (Image Patch)	ViT-L/14	<b>34.9</b>	34.6	35.6	35.1

ViT-B/16 and  $672 \times 672$  for ViT-L/14. We only use image patches for self-distillation. All the other settings remain the same as the experiments on EVA-CLIP ViTs.

**Comprehensive System-Level Comparison.** To provide a thorough and comprehensive system-level comparison of open-vocabulary object detection methods, we present detailed results for both the OV-COCO and OV-LVIS benchmarks in Tab. A5 and Tab. A6, respectively.

#### A.4 USING REGION-TEXT PAIRS

We adopt the methodology proposed in RegionCLIP (Zhong et al., 2022) to fine-tune CLIP ViTs using pseudo-labelled region-text pairs. Specifically, we parse object nouns from the COCO Caption dataset (Chen et al., 2015) and generate region proposals using an RPN trained on COCO’s 48 base categories. To establish correspondence between object nouns and region proposals, the original RegionCLIP extracts region features from the dense feature maps of CLIP CNNs. Differently, we use the image-level features of the image crops enclosing the regions, considering the inferior dense representation of the original CLIP ViT. For a fair comparison, we also fine-tune the model on the train2017 split of COCO dataset (Lin et al., 2014) for the same 6 epochs.

#### A.5 VISUALIZATION

**Open-vocabulary Object Detection.** We present qualitative results for open-vocabulary object detection on the OV-COCO benchmark in Fig. A2. The red boxes indicate novel categories, while the blue boxes represent base categories. These visualizations offer insights into the model’s performance and its ability to detect novel objects.

**Open-Vocabulary Image Segmentation.** We present visualizations of open-vocabulary semantic segmentation results in Fig. A3. The segmentation model is trained on COCO Stuff and evaluated on the ADE20K dataset (Zhou et al., 2017).

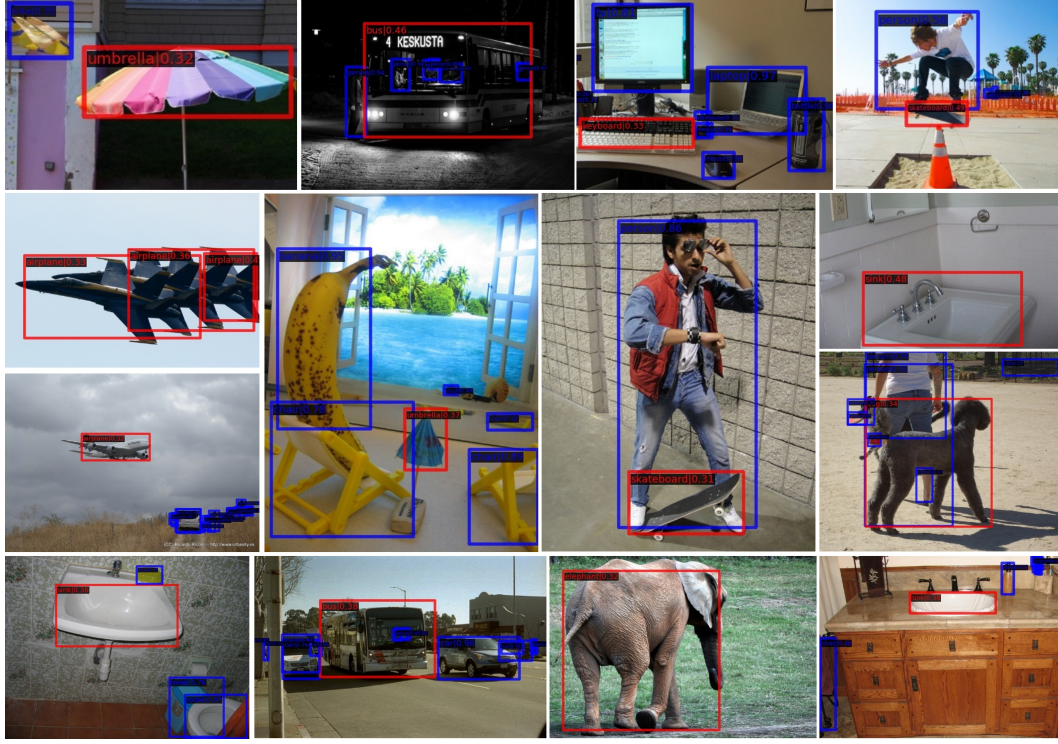


Figure A2: Visualization of image segmentation results. The red boxes are for the novel categories and the blue boxes are for the base categories.



Figure A3: Visualization of image segmentation. The images are from ADE20k (Zhou et al., 2017).

## B BROADER IMPACT & LIMITATION

**Board Impact.** Our work contributes to an in-depth analysis of the dense representation of ViT-based CLIP models and introduces CLIPSelf, an effective approach to unleash the power of CLIP ViTs for open-vocabulary dense prediction. We are the first to build open-vocabulary object detectors upon frozen CLIP ViT backbones and achieve state-of-the-art performance. As transformers are becoming increasingly popular as a unified architecture for both vision and language tasks, it is of great significance to successfully adapt the generalization ability of CLIP ViTs from image classification tasks to dense prediction tasks.

**Limitation.** Our work is built upon the pre-trained CLIP models. Therefore, the performance of CLIPSelf is greatly influenced by the visual-language alignment in the original CLIP models.